AD-A112 234 COLORADO STATE UNIV FORT COLLINS DEPT OF ATMOSPHERI--ETC F/G 4/2
A QUANTITATIVE TECHNIQUE FOR SHORT RANGE WEATHER FORECASTING US--ETC(U)
MAR 81 N E BUSS F19628-78-C-0207

UNCLASSIFIED AFGL-TR-81-0206 NL

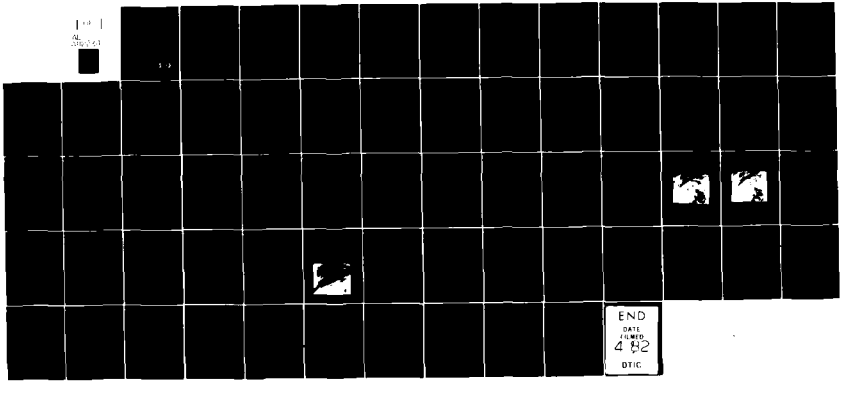

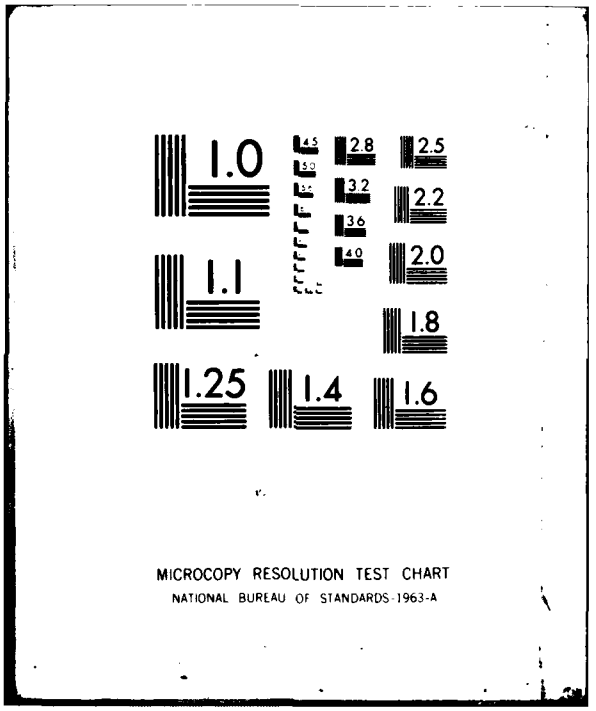
1.0
1.1
1.25
1.4
1.6
1.8
2.0
2.2
2.5
2.8
3.2
3.6
4.0
4.5
5.0
MICROCOPY RESOLUTION TEST CHART
NATIONAL BUREAU OF STANDARDS-1963-A

AFGL-TR-81-0206

A QUANTITATIVE TECHNIQUE FOR SHORT RANGE WEATHER FORECASTING USING NUMERICAL WEATHER PREDICTION GUIDANCE AND DIGITAL SATELLITE IMAGERY

Norman E. Buss

Colorado State University
Atmospheric Science Department
Ft. Collins, Colorado 80523

Scientific Report No. 3

March 1981

AIR FORCE GEOPHYSICS LABORATORY
AIR FORCE SYSTEMS COMMAND
UNITED STATES AIR FORCE
HANSCOM AFB, MASSACHUSETTS 01731

Unclassified

SECURITY CLASSIFICATION OF THIS PAGE (When Data Entered)

REPORT DOCUMENTATION PAGE	READ INSTRUCTIONS BEFORE COMPLETING FORM
1. REPORT NUMBER: AFGL-TR-81-0206	2. GOVT ACCESSION NO.: AD-A112 234 / 3. RECIPIENT'S CATALOG NUMBER:
4. TITLE (and Subtitle): A Quantitative Technique for Short Range Weather Forecasting Using Numerical Weather Prediction Guidance and Digital Satellite Imagery	5. TYPE OF REPORT & PERIOD COVERED: Scientific Report No. 3
	6. PERFORMING ORG. REPORT NUMBER:
7. AUTHOR(s): Norman E. Buss	8. CONTRACT OR GRANT NUMBER(s): F19628-78-C-0207
9. PERFORMING ORGANIZATION NAME AND ADDRESS: Colorado State University, Atmospheric Science Department, Ft. Collins, Colorado 80523	10. PROGRAM ELEMENT, PROJECT, TASK AREA & WORK UNIT NUMBERS: 62101F, 667008AA
11. CONTROLLING OFFICE NAME AND ADDRESS: Air Force Geophysics Laboratory, Hanscom AFB, MA 01731, Monitor/H. Stuart Muench/LYU	12. REPORT DATE: March 1981
	13. NUMBER OF PAGES: 63
14. MONITORING AGENCY NAME & ADDRESS(if different from Controlling Office)	15. SECURITY CLASS. (of this report): Unclassified
	15a. DECLASSIFICATION/DOWNGRADING SCHEDULE

16. DISTRIBUTION STATEMENT (of this Report)

Approved for public release; distribution unlimited

17. DISTRIBUTION STATEMENT (of the abstract entered in Block 20, if different from Report)

18. SUPPLEMENTARY NOTES

19. KEY WORDS (Continue on reverse side if necessary and identify by block number)

Interactive Image Display System
FO-CASTING
Now Casting
LFM
Short Range Terminal Forecasting

20. ABSTRACT (Continue on reverse side if necessary and identify by block number)

A method is outlined to test the concept of "Focasting", proposed by Vonder Haar, et al. (1979), by comparing forecast cloud fields to existing satellite observed cloud fields to examine the accuracy of the forecast. Forecast cloud fields are derived from a set of multiple linear regression coefficients which can then be used to predict what the cloud field should look like at a given forecast valid time, say at one hour intervals from

(Continued on reverse side)

DD FORM 1 JAN 73 1473

Unclassified

SECURITY CLASSIFICATION OF THIS PAGE (When Data Entered)

20. Abstract (Continued from reverse side)

the LFM base time out to 12 hrs. Then by comparing real-time satellite imagery, as it is received at one hour intervals, to the corresponding estimated satellite product (ESP) that was produced from the regression equations, the forecaster can see how well the forecast cloud field fits the actual satellite imagery. The positioning of the forecast cloud field can then be adjusted, based on the deviation from the observed satellite field.

ABSTRACT

A technique was developed to monitor numerical weather prediction output with hourly digital satellite data. The technique is applicable to FOCASTING or Focused Nowcasting using a mix of numerical forecast output, geostationary satellite data, and conventional observations. The process allows the forecast team to focus on areas of significant weather events, then integrate the current satellite observation with the 12 and 24 hour numerical guidance to produce a terminal forecast.

The numerical prediction information is used to produce an Estimated Satellite Product (ESP). The ESP is created by inputting the Limited Area Fine Mesh (LFM) observed and forecast data into a linear regression equation to produce a prediction equation for the existance of a cloud field that would be viewed by a satellite. The regression equations are developed by a stepwise procedure in which the predictand is the infrared radiative temperature observed by the GOES East Satellite. The predictors are made up of parameters that best represent the existence of a cloud, and are computed from LFM forecast data. Equations are developed for three tropospheric layers representing low, middle and high cloud regions. The regression equations developed are for a limited case of the early winter season.

The ESPs are developed for each hour of the forecast period by interpolation of LFM output. The ESP is displayed on the CSU ADVISAR in the same resolution and earth navigation system as the GOES imagery. This permits precise comparison between the LFM derived estimated satellite product and the actual GOES image for the same valid time. The

forecaster can isolate an active weather system by displaying a mesoscale window of the LFM grid network.

Several case studies are examined to demonstrate the feasibility of the ESP/Satellite mix in forecasting the onset and duration of ceiling height categories and precipitation.

TABLE OF CONTENTS

1.0 INTRODUCTION

1.1 The Operational Forecast Problem

Prior to 1970, operational forecasters tasked with providing time specific, terminal aviation forecasts (TAFs) encountered a three-fold problem: 1) an observational data base with large distances between observing sites; 2) a large amount of available data, but received in the often cumbersome form of facsimile maps and teletype printouts; 3) little time in which to mentally integrate the vast amount of numbers and charts in a high pressure environment. With the advent of operational geostationary meteorological satellites in the mid 1970's the first problem was at least alleviated, since the SMS/GOES satellite observing platforms provide a continuous spatial domain of cloud fields in a near time continuous domain of hourly or half hourly transmission. The second problem is being treated by the use of advancing electronics through the development of automated weather data distribution and display systems. In addition to addressing the cumbersome data problem, these devices also allow more time for forecast development through the rapid transmission and analysis of meteorological parameters, therefore addressing the third problem. The National Weather Service is currently bringing such a device into operations under a program entitled the Automation of Field Operations and Services or AFOS (Klein, 1978). Such a system will eliminate the need for most teletypewriter and facsimile machines in Weather Service Forecast offices. Through the use of minicomputers and cathode ray devices, maps, charts, diagrams and alpha numeric displays can be readily generated from existing data sources. Similar systems are planned by both Air Weather Service and the Naval Office of Oceanography and Meteorology.

It would be useful, then, to develop an operationally compatible system in which satellite data could be included in the man-machine forecast display system with conventional meteorological data.

This natural mesh of conventional data with real time satellite observations would allow the forecaster to integrate a large spectrum of meteorological data into his or her analysis and forecasting routine. The purpose of this paper is to propose and test a method for the forecaster to use real time geostationary satellite data along with the existing numerical weather prediction products in an interactive, yet quantitative, manner to improve the accuracy and timing of the short-term forecast.

1.2 The Data Selection

Two forecast tools that have gained wide acceptance in the forecasting community are fine resolution numerical weather prediction output and meteorological satellite imagery data. The two primary forms of these products currently in use are the Limited Area Fine Mesh (LFM-II) numerical weather prediction model and the infrared and visible satellite imagery from the Geostationary Operational Environmental Satellite (GOES) systems.

The use of these tools in tandem would be beneficial in the aspect of maximizing the effectiveness of each product. The LFM provides a relatively high degree of confidence in computing the future movement and development of dynamic weather systems. The GOES imagery provides time consistent, hourly or half hourly, spatially contiguous observations of existing dynamic features through cloud pattern images. Therefore, these two data types in conjunction with conventional surface

observations could provide the forecaster with an excellent new data base for preparation of short range terminal forecasts.

One complication in dealing with these two data types is the vast amount of information that must be processed. For example, for each 12 hour period the following amounts of data were available for this study. The available LFM output totaled 85,888 data elements for the three forecast periods required. The digital GOES infrared data was comprised of $5x10^5$ data elements each hour, or $6x10^6$ data elements for every 12 hour period. Obviously computer assistance is manditory in dealing with this magnitude of numbers. For research purposes the Colorado State University, Department of Atmospheric Science, ADVISAR (All Digital Video Interactive System for Atmospheric Research) meets the hardware requirements necessary for this type of work.(1)

1.3 Previous Meteorological Research Incorporating Model Output, Satellite Data and Man Interactive Computer Systems

The concept of using satellite observation in conjunction with numerical models for use in mesoscale forecasting was proposed (Kreitzburg, 1976) as a feasible technique for the 1980's. In a discussion of interactive system requirements for mesoscale weather detection and prediction (Anthony and Bristor, 1978), satellite data inputs and conventional data inputs (including basic surface and rawinsonde observations in addition to numerical weather products) were listed among the

---

(1) The ADVISAR configuration at the time of this research consisted of a Digital Equipment Corporation PDP 11/60 minicomputer, a digital video display subsystem consisting of eight 512x512 memory planes with eight bit (256) resolution, two nine track tape drives, a 300 mega-byte disk and color television monitors.

primary requirements for future nowcasting facilities.

The research community has applied the use of satellite data, meshed with a wide variety of conventional data and data analysis techniques, toward the mesoscale weather prediction problem using man interactive video display systems.

These applications include the use of time consecutive satellite observation of cloud fields to determine mesoscale cloud motion fields (Leese, et al., 1971; Smith and Phillips, 1972; Muench and Hawkins, 1979; Demasters and Brown, 1979; Haass and Brubaker, 1979; Smith and Vonder Haar, 1980; Vonder Haar, 1980; and Muench, 1980). These techniques all basically use a time series of satellite cloud fields to produce cloud movement prediction, and do not incorporate any dynamic forecast information.

Statistical correlations of satellite data with various meteorological data has been widely published. Satellite radiation measurements (from TIROS satellites) were used as predictors of synoptic meteorological data by Lethbridge and Panofsky (1969). Using combinations of the water vapor channel, the infrared channel and the visible channel, skill was demonstrated in predicting the probability of precipitation and thunderstorms in addition to relative humidity values, low ceilings, cloud amounts and vertical motion. In an attempt to input satellite data into numerical analysis and prediction, satellite observed cloud patterns were demonstrated to be useful in modifying 500 mb height fields (Nagle and Clark, 1968). This study developed relationships between satellite observed spiral cloud patterns and 500 mb height fields through the use of multiple linear regression equations.

Statistical applications of satellite data towards improvement of short range forecasts were first attempted with early ATS-3 visible satellite imagery (Sikula and Vonder Haar, 1972). Their early work demonstrated skill in predicting parameters of ceiling and total opaque cloud cover for short time periods by incorporating satellite brightness as a predictor in multiple linear regression equations. Follow on work by Conover (1974) improved the ceiling prediction statistics of Sikula and Vonder Haar by categorizing the probability of clouds by levels.

Satellite data in conjunction with digital radar data has been demonstrated as a useful analysis technique using the data composite concept (Reynolds and Smith, 1979). Digital GOES imagery in conjunction with rawinsonde data has been shown to be useful in observing and detecting severe hail storms (Reynolds, 1980) and in the study of rain bands in extratropical cyclones (Kruidenier, 1980).

Interactive computer systems have been demonstrated to be useful in depiction of forecast convective areas using satellite and conventional data (Wash, et al., 1979). Recently atmospheric scientists at the University of Wisconsin, SSEC (Wash and Whittaker, 1980), developed advection forecasting algorithms to fill the gap between standard upper air observation times and the availability of LFM 12 hour forecasts. The results of these algorithms were graphically displayed on a man-interactive imaging system. The use of conventional meteorological data fields graphically overlayed on digital satellite data was demonstrated as a useful weather analysis tool and capable of improving accuracy of forecasting (Suchman, et al., 1978) when displayed as a data composite.

LFM-II guidance has been used in several studies applying satellite data. A computerized techinque was developed (Wilson, 1978) which used

LFM model variables to predict location and severity of thunderstorms, using satellite imagery and radar information to verify the results. The use of satellite data to fine tune LFM numerical guidance was demonstrated in two severe storm cases by the NOAA, NESS, Satellite Field Service Station, Kansas City, Missouri (Ferguson and Matthews, 1978). Such work was a forerunner to the standard issuance of satellite interpretation bulletins by SFSS groups. These guidance products, however, do not apply a computer graphics display system to mix the two data types, nor do they use computer based quantitative algorithms to obtain a forecast or guidance.

In a study on estimating infrared radiation flux density at the top of the atmosphere, Jensenius, Cahir, and Panofsky (1978) used LFM model output to develop predictor variables of radiative flux observed by the NOAA-3 satellite. Their technique involved developing a regression equation with the observed satellite radiant flux as the predictor and the predictors derived from the LFM output. The predictors used in the study were derived as variables which were believed to be associated with cloudiness and temperature.

1.4 The Concept of Estimated Satellite Products

This study was designed to test the concept of Focasting or Focused Nowcasting proposed by Vonder Haar, et al. (1979). Essentially this process involves a comparison of forecast cloud regions with a high resolution nowcast (existing satellite imagery and conventional meteorological observations) as part of the data mix entering into short range forecasting development. This method allows the forecaster to focus on areas in which discrepancies are noted between the satellite nowcast and the forecast cloud features. These discrepancies may include such items

as the horizontal displacement of cloud features, the spatial orientation and coverage of cloud masses, the vertical extent of cloud elements, and the existence of cloud regions. Sound meteorological interpretation of the nowcast/forecast combination would then be a viable asset in development of subsequent forecasts.

There are several possibilities available by which to quantize the bridge between numerical weather prediction products and satellite imagery for meteorological analysis and forecasting. One method would be to use cloud motion wind fields derived from satellite imagery in comparison with wind fields forecast by numerical guidance. A second possibility would be to compare observed satellite imagery and forecast fields with respect to "centers of action", i.e. cloud masses on the imagery and LFM forecast geopotential height patterns, or observed frontal cloud bands and forecast thickness gradients. Another approach would be to use a cloud dynamics model. with LFM forecast fields as input, which would reflect cloud features. This would be used as a method for comparing the vertical and horizontal extent of forecast and observed cloud regions.

Because the FO-CAST concept would benefit from a time interpolation of LFM fields for better timing resolution, large quantities of data are involved. Thus a simple method of bridging the numerical weather prediction/satellite gap was desired. Jensenius, et al. (Ibid), inspired a conceptual design which would allow for rapid computer application of the large quantities of LFM and satellite data required for each forecast period. The approach of the present study, then, was to apply the LFM forecast fields as variables in multiple linear regression equations which predict cloud features as viewed from geostationary satellites.

For this study it was decided to develop a set of linear regression equations derived from numerical weather prediction produced by the LFM-II model as predictors and GOES-East digital satellite infrared (IR) values as the predictands. These equations, then, when applied to a set of LFM data would produce a data file of predicted satellite IR values. This file when graphically displayed on a computer video screen would then be a numerical estimate of the satellite observed IR signature at the LFM forecast valid time. This LFM satellite derived product will henceforth be regarded as an Estimated Satellite Product or ESP. If an ESP is developed for the initial, or analyzed, fields on which the LFM run is based, it could provide useful information to the forecaster when compared to the satellite image for the same valid time. This would be especially useful if the satellite image and the ESP were displayed in the same coordinate system and the same resolution, allowing for the rapid identification of discrepancies between the two products. By use of interactive computer methods, the video display of the memory frames containing a series of ESPs and satellite imagery could be looped or meshed (i.e. split frame display) for comparison by the forecaster. Such vital analysis by the forecaster could then be used to determine the validity of the analysis fields with respect to cloud features observed on the imagery. This information may suggest to the forecaster areas in which the LFM forecasts may be in error due to misplacement of dynamic features. Examples may include the location of vorticity centers, placement of frontal zones, the location of cyclone centers, and the location and/or existence of short baroclinic waves. The forecaster, then, could formulate his forecast by including mental (or actual interactive bogus) adjustments to the predicted location cloud

system location and development based on the discrepancies and/or agreements of the ESP and satellite image mix.

To further test the applicability of the ESP concept to the short range forecast problem, ESPs will be developed for successive hourly increments by interpolation of input LFM data. For example, given a 0000 GMT analysis LFM data set and the corresponding 12 hour forecast LFM data set (i.e. based on 0000 GMT valid at 1200 GMT), a series of 12 ESPs can be produced. Due to a data computation and transmission lag, this information would not be available to the operational forecaster until 0230 GMT. By 0300 GMT this data could be applied to the ESP production giving, for example, the following ESPs: 03Z, 04Z, 05Z, 06Z, 07Z, 08Z and 09Z, thus providing the next 6 hours of ESP guesses to the cloud fields. At this point the ESPs could be used along with the current GOES imagery (i.e. up to and including the 0300Z data), for the next 6 hour short range forecast.

This stage of operations will, however, require the forecaster to mentally integrate the areas of discrepancies and/or agreements between the most recent GOES image and the coinciding valid ESP, and mentally extrapolate the descrepancies to the remaining ESPs of the forecast series. The ultimate goal of this type of data mix should be to BOGUS the ESP with the satellite observed cloud fields to provide a series of improved "second guess" ESPs for the forecast period. The bogusing would be aided by quantitative comparison between ESPs and actual real time GOES digital images. Such quantitative guidance allows the FOCAST concept to be implemented.

2.0 RESEARCH OBJECTIVES

2.1 Objectives

The primary objective of this research effort is to develop a system which incorporates numerical weather prediction output and digital satellite data into a new, efficient tool for mesoscale analysis and short range forecasting. This is accomplished by developing a computer graphic display of forecast cloud fields from a numerical weather prediction model output which can be manually compared to satellite imagery displayed in a similar reference frame.

Key considerations in the development of this approach are:

1) To provide a system not dependent on the diurnal availability of visible satellite imagery.

2) To make computational requirements and data storage requirements acceptable for use with minicomputer display systems.

2.2 Research Approach

Using a compatible set of Limited Area Fine Mesh numerical model output and digital infrared data from a geostationary satellite, a set of regression equations is being developed which predict effective mean radiative temperature fields, as viewed from the satellite sensors. This required the development of a data reduction program which uses model output parameters to produce a set of variables that are associated wih cloudiness.

The predictands in the multiple linear regression equations development were the mean infrared satellite brightness counts, converted to effective blackbody irradiance temperatures at the LFM grid

model's points. This required the development of a satellite analysis program that samples the infrared image around each LFM grid point location.

The next step in the research effort is to determine the statistical reliability of the multiple linear regression equations by testing them on an independent sample of LFM and infrared satellite data.

Finally, by using selected case studies, tests will be conducted to determine the feasibility of this approach to mesoscale analysis and short range aviation forecasting events. This requires developing a technique for video display of the regression equation results such that it can easily be compared with similar displays of satellite data.

3.0 DATA ACQUISITION AND REDUCTION

3.1 Limited-Area Fine Mesh Model Data

3.1.1 Model Description

The numerical weather prediction data used in this study was computed at the National Meteorological Center (NMC) using the Limited-Area Fine Mesh (LFM-II) model. A comprehensive description of this model is given in National Weather Service Technical Procedures Bulletin No. 232 (Rieck, 1978). The LFM-II model became operational in 1977, replacing a similar model (LFM-I) which had a larger computational grid increment. It produces operational forecasts for 48 hours beyond the data base initiation times of 0000 GMT and 1200 GMT. The computational grid covers an area which includes most of North America and adjacent ocean areas. The grid array is 79 x 67, on a polar sterograhic map projection true at 60^{o} North latitude and centered at 105^{o} West longitude. The computational grid distance is 116 km at 45^{o} North, but the output parameters are produced on the preceeding LFM model's (LFM-I) grid array, which contains a grid resolution of 174 km at 45^{o} North (Brown, 1977).

The model's vertical stratification consists of six layers: a planetary boundary layer, 50 mb in depth; three tropospheric layers, each one third of the depth from the top of the planetary boundary layer to the tropopause; and two stratospheric layers. A final, constant potential temperature, layer is added at the top for computational reasons. The vertical surfaces on which the calculations are made are Sigma surfaces, where σ is defined (Shuman and Hovermale, 1968) as:

$$\sigma = \frac{P - P_u}{P_L - P_u} \qquad (1)$$

where P is the pressure level in question and P_U and P_L represent the pressure levels above and below P, respectively.

The LFM solves a set of eight finite difference equations in time increments of 360 seconds, with five quantities being carried forward in time: the u wind component, the v wind component, the layer mean temperature, the layer pressure thickness and the precipitable water.

The computed output data is finally returned from the sigma surfaces to constant pressure surfaces by interpolation.

3.1.2 LFM Data Acquisition

Model output for this research was obtained through the Water and Power Resource Service (WPRS), Skywater environmental data network. The WPRS data base was used since the Colorado State University's ADVISAR system has a dedicated communications and data acquisition link to the WPRS data storage facilities. The use of this data base, then, will provide for further research capabilities based on this work which may require real-time data acquisition testing. A complete description of the WPRS data network is available in the Project Skywater Environmental Data Network Users Manual, revised January, 1980.

The LFM data available at the WPRS consists of the initial data fields (analysis) in addition to the 12 and 24 hour forecast fields for a given date-time group. The grid of the data points is given in Figure 1. This grid contains a 22 x 32 array on a polar stereographic map projection true at 60° North. This grid is a subsection of the entire LFM output grid described in section 3.1.1 (i.e. 22 x 32 vs. 53 x 45). The grid interval is 190.5 km at 60° North, 105° West.

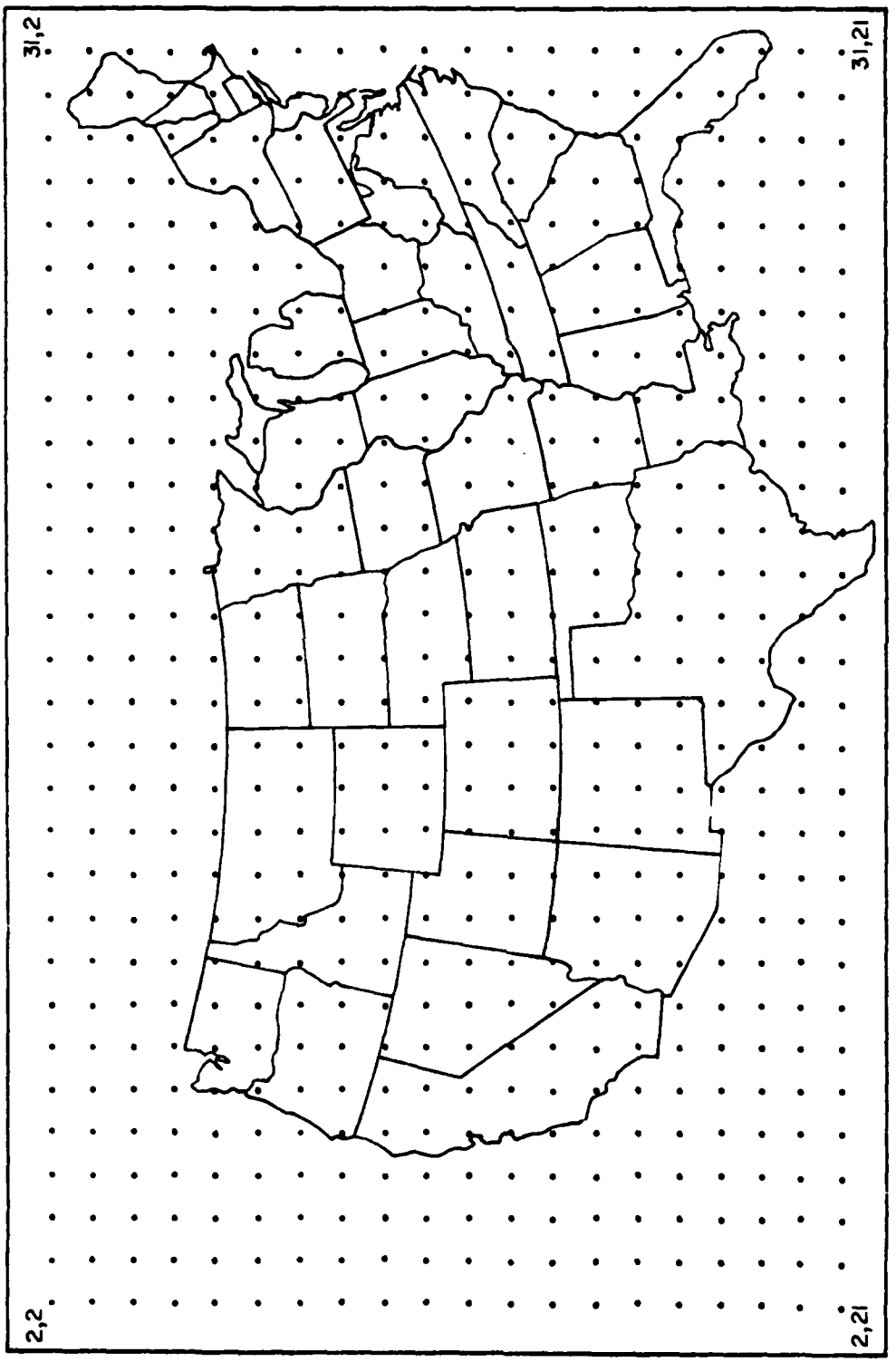

LOCATION OF WPRS GRID POINTS

Figure 1.

The data were obtained on magnetic tape on the WPRS CDC CYBER system. Table 1 lists the data fields requested for the initial, or analysis, data sets and Table 2 lists the data fields requested for the 12 and 24 LFM forecast data sets. The units of the LFM fields are as follows:

Temperature: Degrees Kelvin (^{o}k)

Dew Point Temperature: Degree Kelvin (^{o}k)

Heights of Pressure surface: Geopotential Meters (m)

Wind Components: Meters Per Second (ms^{-1})

Vertical Motion: Millibars Per Second ($mb\ s^{-1}$)

Note that no vertical motion fields are available for the initial data times.

Data were requested for November 1-30, 1979 and November 1-30, 1980. The November 1979 data set represents the dependent sample data base for the ESP multiple linear regression equations, with November 1980 representing the independent sample data base. Data were requested for 114 fields (i.e. 1000 mb temperature, 850 mb temperature, etc.) for each date time group of the two month period. Due to data transmission difficulties or the inability of the binary data to be unpacked, many fields were not available. Additionaly, none of the November 1980 24 hour forecast information was available. Table 3 summarizes the collected fields for the 1979 data set and Table 4 summarizes the 1980 LFM data set.

The LFM model is run twice a day, for both the 0000 GMT and 1200 GMT observations. Therefore there was 60 potential date/time groups for each of the November data sets, with 114 desired field arrays each. Of the total 6840 desired fields for each November data set, approximately

Table 1

LFM INITIAL DATA FIELDS AVAILABLE ON TAPE

Pressure Level	Field Name	Pressure Level	Field Name
1000 mb	00TT0	400 mb	40TT0
	00TD0		40TD0
	00HH0		40HH0
	00UU0		40UU0
	00VV0		40VV0
850 mb	85TT0	300 mb	30TT0
	85TD0		30TD0
	85HH0		30HH0
	85UU0		30UU0
	85VV0		30VV0
700 mb	70TT0	250 mb	25TT0
	70TD0		25HH0
	70HH0		25UU0
	70UU0		25VV0
	70VV0		
		200 mb	20TT0
500 mb	50TT0		20HH0
	50TD0		20UU0
	50HH0		20VV0
	50UU0		
	50VV0		

Legend: The characters in the field name correspond to the following meteorological variables:

TT	Temperature Field
TD	Dew Point Temperature Field
HH	Geopotential Height Field
UU	"u" Wind Component Field
VV	"v" Wind Component Field

Table 2

LFM 12 and 24 Hour Forecast Data Fields Available On Tape

Pressure Level	Field Name	Pressure Level	Field Name
1000 mb	00TT1	400 mb	40TT1
	00TDL		40TD1
	00HH1		40UU1
	00UU1		40VV1
	00VV1		
	00WW1	300 mb	30TT1
			30TD1
850 mb	85TT1		30UU1
	85TD1		30VV1
	85HH1		
	85UU1	200 mb	25TT1
	85VV1		25UU1
	85WW1		25VV1
700 mb	70TT1	250 mb	20TT1
	70TD1		20UU1
	70HH1		20VV1
	70UU1		
	70VV1		
	70WW1		
500 mb	50TT1		
	50TD1		
	50HH1		
	50UU1		
	50VV1		
	50WW1		

Legend: The characters in the field name correspond to the following meteorological variables:

TT	Temperature Field
TD	Dew Point Temperature Field
HH	Geopotential Height Field
UU	"u" Wind Component Field
VV	"v" Wind Component Field
WW	Vertical Motion Field

Table 3

1979 LFM Data Collection Summary

Date	Time (GMT)		Number of Fields
1 Nov	0000	All Missing	0
	1200	Initial Missing, 12 HR Missing, 24 HR Available	38
2 Nov	0000	85UU0 Missing	113
	1200	All Available	114
3 Nov	0000	30TD1 Missing	113
	1200	All Available	114
4 Nov	0000	All Fields Available	114
	1200	All Fields Available	114
5 Nov	0000	30TD1 Missing	113
	1200	70TT0 Missing	113
6 Nov	0000	All Fields Available	114
	1200	All Fields Available	114
7 Nov	0000	All Fields Available	114
	1200	50TT2 Missing	113
8 Nov	0000	All Fields Available	114
	1200	70WW1 Missing	113
9 Nov	0000	50WW2 Missing	113
	1200	25HH0, 00TD2 Missing	112
10 Nov	0000	All Fields Available	114
	1200	All Fields Available	114
11 Nov	0000	All Missing	0
	1200	All Fields Available	114
12 Nov	0000	30TD1, 85VV2 Missing	112
	1200	*70WW2 Bad Data	114
13 Nov	0000	All Fields Available	114
	1200	All Initial Data Missing	0
14 Nov	0000	All Fields Available	114
	1200	25WW1 Missing	113
15 Nov	0000	All Fields Available	114
	1200		

Table 3 -- Continued

Date	Time (GMT)		Number of Fields
16 Nov	0000	70VV0 Missing	113
	1200	70UU0 Missing	113
17 Nov	0000	All Fields Available	114
	1200	All Fields Available	114
18 Nov	0000	25UU1 Missing	113
	1200	All Fields Available	114
19 Nov	0000	All Fields Missing	0
	1200	All Fields Available	114
20 Nov	0000	70TT1, 20TT1, 85VV2 Missing	111
	1200	23 Fields Missing for Initial Data	91
21 Nov	0000	All Fields Available	114
	1200	00WW1 Missing	113
22 Nov	0000	All Initial and 12 HR Forecasts Missing	38
	1200	All Initial and 12 HR Forecasts Missing	38
23 Nov	0000	All Initial and 12 HR Forecasts Missing	38
	1200	All Initial and 12 HR Forecasts Missing	38
24 Nov	0000	All Initial and 12 HR Forecasts Missing	38
	1200	00HH0 Missing	113
25 Nov	0000	All Fields Available	114
	1200	All Fields Available	114
26 Nov	0000	All Fields Available	114
	1200	85TTZ Missing	113
27 Nov	0000	All Fields Available	114
	1200	00VVD, 85TT0 Missing	112
28 Nov	0000	All Fields Available	114
	1200	40TT0, 50VV1 Missing	112
29 Nov	0000	All Fields Available	114
	1200	All Fields Available	114
30 Nov	0000	All Fields Available	114
	1200	All Fields Available	114
		TOTAL	6,031

Summary

88% of desired total number of fields

Table 4

1980 LFM Data Collection Summary

Note: 24 Hour Forecasts Were Not Available

Date	Time (GMT)		Number of Fields
1 Nov	0000	All Fields Missing	0
	1200	All Fields Missing	0
2 Nov	0000	All Fields Missing	0
	1200	All Fields Missing	0
3 Nov	0000	24 Hr Forecasts Missing	76
	1200	24 Hr Forecasts Missing	76
4 Nov	0000	All Fields Missing	0
	1200	All Fields Missing	0
5 Nov	0000	24 Hr Forecasts Missing	76
	1200	24 Hr Forecasts Missing	76
6 Nov	0000	20VV1, 24 Hr Forecasts Missing	75
	1200	30TT0, 24 Hr Forecasts Missing	75
7 Nov	0000	00WW1, 24 Hr Forecasts Missing	75
	1200	01UU0, 50HH1 Missing	74
8 Nov	0000	24 Hr Forecasts Missing	76
	1200	24 Hr Forecasts Missing	76
9 Nov	0000	24 Hr Forecasts Missing	76
	1200	24 Hr Forecasts Missing	76
10 Nov	0000	All Fields Missing	0
	1200	24 Hr Forecasts Missing	76
11 Nov	0000	24 Hr Forecasts Missing	76
	1200	All Data Missing	0
12 Nov	0000	All Data Missing	0
	1200	24 Hr Forecasts Missing	76
13 Nov	0000	24 Hr Forecasts Missing	76
	1200	24 Hr Forecasts Missing	76
14 Nov	0000	50HH0 Missing	75
	1200	24 Hr Forecasts Missing	76
15 Nov	0000	24 Hr Forecasts Missing	76
	1200	85TT1 Missing	75

Table 4 -- Continued

Date	Time (GMT)		Number of Fields
16 Nov	0000	All Fields Missing	0
	1200	All Fields Missing	0
17 Nov	0000	All Fields Missing	0
	1200	All Initial and 24 Hr Fields Missing	38
18 Nov	0000	24 Hr Forecasts Missing	76
	1200	30UU0 Missing	75
19 Nov	0000	24 Hr Forecasts Missing	76
	1200	24 Hr Forecasts Missing	76
20 Nov	0000	24 Hr Forecasts Missing	76
	1200	24 Hr Forecasts Missing	76
21 Nov	0000	24 Hr Forecasts Missing	76
	1200	All Fields Missing	0
22 Nov	0000	All Initial and 24 Hr Forecasts and 50TT1 Missing	37
	1200	24 Hr Forecasts Missing	76
23 Nov	0000	24 Hr Forecasts Missing	76
	1200	24 Hr Forecasts Missing	76
24 Nov	0000	All Fields Missing	0
	1200	24 Hr Forecasts Missing	76
25 Nov	0000	30HH0 Missing	75
	1200	24 Hr Forecasts Missing	76
26 Nov	0000	70VV0, 25HH0 Missing	74
	1200	24 Hr Forecasts Missing	75
27 Nov	0000	All Fields Missing	0
	1200	40HH0, 24 Hr Forecasts Missing	75
28 Nov	0000	24 Hr Forecasts Missing	74
	1200	24 Hr Forecasts Missing	76
29 Nov	0000	24 Hr Forecasts Missing	76
	1200	24 Hr Forecasts Missing	76
30 Nov	0000	24 Hr Forecasts Missing	76
	1200	24 Hr Forecasts Missing	76

Summary

TOTAL 3,331

48% of desired total number of fields

73% of initial and 12 hr forecasts

88% of the November 1979 and 48% of the November 1980 set was collected. Each data set acquired represents at least 3.5×10^6 grid point values.

3.1.3 LFM Data Reduction

The intent of the first-guess ESP is to produce a forecast of cloud fields by the use of multiplier linear regression equations having LFM output as the predictor variables. The raw LFM output is not in itself useful as predictors or indicators of cloudiness or cloud free regions, on the grid. Therefore, it was necessary to produce from the raw LFM output, a sufficient number of variables which have some meterological semblance to cloudiness. To enhance the vertical resolution of the cloudiness predictors it was decided to develop three separate sets of predictor equations, representing low, middle and high cloud regions for each LFM forecast type; the initial analyses, the 12 hour forecast and 24 hour forecast. The low cloud predictors contain data from 1000 mb, 850 mb and 700 mb. The middle cloud predictors contain 700 mb and 500 mb data inputs and the high cloud predictors contain data input from 500 mb to the 250 mb fields. Although 200 mb data was acquired, it never appeared in the predictor equations, mainly because 200 mb was considered above the mean tropopause for the season and grid area concerned.

Appendix A summarizes the LFM predictors developed from the raw LFM fields.

Appendix B summarizes the equations used in development of the LFM predictors.

3.1.3.a Predictors Based on Low Dew Point Depression

Low dew point depressions have been used as a simple, yet effective, nephanalysis tool for many years. Dew point depression equal to or less than $5^{\circ}C$ were used to cut-off criterion for the levels from 1000 mb to 500 mb. Dew point depressions of $10^{\circ}C$ or less were used as cut-off criterion at the 400 mb and 300 mb levels. The increased dew point depression cut-off at the higher levels was justified by personal observation and can be physically related to consideration of the frost points associated with the upper troposheric temperatures. The dew point depression itself was not used as predictor variable, but instead, the temperature of the grid point became the variable when the low dew point criteria was met. Since the predictand of the regression equations is a mean temperature value and the goal in applying the resultant regression equation was to produce an effective cloud temperature field, it was hoped that the use of the temperature field would reduce the variance associated with this type of a predictor. Similar considerations were used in other variables entering the multiple linear regression scheme.

For situations in which none of the three low levels contained a low dew point depression, an effective surface temperature was calculated. For such grid point locations with mean sea level elevations the 1000 mb temperature was returned as the low "cloud" predictor. For grid point locations with elevations greater than sea level the surface temperature was calculated by reversing the techniques used to compute the 1000 mb temperature in the actual model run (Stackpole, 1970). Thus, the surface temperatures of the non-sea level grids were

calculated by using a standard lapse rate "through" the terrain of 6.5°C km^{-1}, the 1000 mb geopotential height, and the grid point elevation. The elevation data was interpolated from the LFM topography (Rieck, 1979).

3.1.3.b Predictors Based on High Relative Humidity

Regions of high relative humidity are associated with cloud regions. Although a given parcel of air must be at, or very near, saturation in order to produce a condensate (in the presence of sufficient cloud condensation nuclei); on the synoptic scale, relative humidities less than saturation are associated with cloud regions. Relative humidities of 60% or greater were used as a definition of cloudiness. This is the same value used in the LFM as a cutoff defining cloud regions for long wave radiative transfer calculations (Rieck, 1978).

For high cloud regions, i.e. 500 mb and above, relative humidity was calculated with respect to ice. This is in agreement with radiosonde data analysis reported by Starr and Cox (1980).

Another variable determined from the relative humidity fields incorporated a temperature weighting function for layers which had a high relative humidity ($\geq 60\%$) at a given level and a low relative humidity ($<60\%$) at the next higher level. This variable, then, attempts to determine an effective cloud top temperature above a moist layer level.

A third variable incorporating relative humidity involved the product of relative humidity and the vertical motion for each of the three cloud types: low, middle and high. Thus, two pre-requisites for cloud formation were mixed — high moisture content and upward vertical motion.

Finally, relative humidity fields in the low layer were averaged and multiplied by the magnitude of the mean low layer wind. It was hoped that this variable would differentiate between regions of high moisture with strong winds (i.e. in the vicinity of cyclones) and regions of low moisture and weak winds (i.e. in the vicinity of surface anticyclones).

3.1.3.c Predictors Based on Vertical Motion

Vertical motion at the grid point was used as a predictor for the following pressure levels: 850 mb, 700 mb, 500 mb. In addition, 400 mb and 300 mb vertical motion fields were also used as predictors in the initial (analysis) equation development. The vertical motion fields for the initial (analysis) data sets were not available from the WPRS data base. Therefore, they were computed by use of the kinematic method, using finite difference approximations for the divergence calculations (Holton, 1979).

Omega, w, the time rate of pressure change:

$$w = \frac{dp}{dt} \tag{2}$$

was assumed zero at the bottom level, 1000 mb, and at the top level, 250 mb. The 250 mb level was chosen as the top since it is a reasonable value for mean tropopause pressure for the area and season in question. To correct for mass balance requirements, corrections to the mean divergence fields in the vertical were applied (Johnson, 1979).

3.1.3.d Predictors Based on Baroclinity

In an attempt to provide a predictor which is associated with regions of frontal zone cloudiness, it was decided to use a variable which reflects frontal dynamic structure. Since frontal zones are

associated with strong thermal gradients in the lowest one half of the troposphere, a predictor which is a function of the thermal gradient could be applied. The thermal wind relation (Holton, 1979):

$$T = \frac{1}{f} (K \times \nabla (\phi_1 - \phi_o)) \tag{3}$$

is such a variable and could easily be computed from the basic data. In order to avoid the use of 1000 mb geopotential height values in high elevation or mountainous regions, the thermal wind was calculated for the 850 mb to 500 mb layer. The magnitude of the thermal wind was the value used as a predictor.

3.1.3.e Jet Stream Cirrus Predictors

Cirrus clouds associated with the polar and subtropical jet streams are useful in frontal analysis of satellite data (Anderson, et al., 1974). In order to parameterize the zones in which jet stream cirrus occurs, the 300 mb wind fields were analyzed for regions of jet strength winds, i.e., wind speeds greater than or equal to 35 ms^{-1}, associated with anticyclonic relative vorticity, where the relative vorticity is defined as:

$$\zeta = \frac{\partial v}{\partial x} - \frac{\partial u}{\partial y} \tag{4}$$

This follows the approach used in a similar study incorporating LFM data reduction (Jensenius, et al., 1978) to parameterize jet cirrus.

3.2 Digital Geostationary Satellite Data Collection and Reduction

3.2.1 GOES Meteorological Satellite Data Acquisition

In order for this research approach to be viable in 24 hour a day applications, only infrared (IR) data was utilized in this study. This eliminated the "daylight only" availability of visible channel satellite data. One drawback to this approach is the inability to determine if a particular region viewed by the IR sensors contains cloud elements or is cloud free. This is a significant problem when dealing with low level cloud tops associated with stratus clouds or fog; in which case the cloud top temperature may be at, or very near, the background (surface), effective radiant temperature. For case study applications, this problem will be addressed by applying surface based observations into the ESP/satellite mix.

The digital satellite data required for this study was collected at the Colorado State University Direct Readout Satellite Ground Station (DRSGS). All data used was retrieved from the GOES-East satellite, which is located in a geosynchronous orbit, with a sub-satellite point near 0^{o} latitude and 75^{o} west longitude. The portion of the full disk image used in this study for the multiple linear regression equation development began at scan line 200 and required approximately 300 scan lines to the south. The east-west elements of the sector provided coverage of the contigious United States. Resolution of the raw IR data was sectorized to magnetic tape in 8 km x 8 km resolution.

The data base for November 1979 was collected at the CSU DRSGS and archived at the National Center for Atmospheric Research (NCAR). The available 0000 GMT and 1200 GMT digital data files were retrieved from the NCAR terabit mass storage device and transfered to 9 track magnetic tape for compatibility with the ADVISAR system. Of the 60 possible 0000 GMT and 1200 GMT data files for the month of November, 48 were obtained.

Table 5: Data collection for multiple linear regression development and testing. A check mark denotes the availability of the image and N/A represents the non-availability of the data.

DATE	TIME	1979	1980	DATE	TIME	1979	1980
1 Nov	0000	✓	N/A	16 Nov	0000	✓	✓
	1200	N/A	N/A		1200	✓	✓
2 Nov	0000	✓	✓	17 Nov	0000	✓	✓
	1200	✓	✓		1200	✓	✓
3 Nov	0000	✓	N/A	18 Nov	0000	✓	✓
	1200	N/A	N/A		1200	✓	✓
4 Nov	0000	✓	✓	19 Nov	0000	✓	✓
	1200	✓	✓		1200	✓	✓
5 Nov	0000	✓	✓	20 Nov	0000	✓	✓
	1200	✓	✓		1200	N/A	✓
6 Nov	0000	✓	✓	21 Nov	0000	✓	✓
	1200	N/A	✓		1200	✓	✓
7 Nov	0000	✓	✓	22 Nov	0000	N/A	✓
	1200	N/A	✓		1200	N/A	✓
8 Nov	0000	✓	✓	23 Nov	0000	✓	N/A
	1200	✓	✓		1200	✓	N/A
9 Nov	0000	✓	✓	24 Nov	0000	✓	N/A
	1200	✓	✓		1200	✓	N/A
10 Nov	0000	✓	✓	25 Nov	0000	✓	✓
	1200	✓	N/A		1200	✓	✓
11 Nov	0000	✓	✓	26 Nov	0000	N/A	✓
	1200	✓	✓		1200	✓	✓
12 Nov	0000	N/A	✓	27 Nov	0000	✓	✓
	1200	✓	✓		1200	✓	✓
13 Nov	0000	N/A	✓	28 Nov	0000	✓	✓
	1200	N/A	N/A		1200	N/A	✓
14 Nov	0000	✓	✓	29 Nov	0000	✓	✓
	1200	✓	✓		1200	✓	✓
15 Nov	0000	✓	N/A	30 Nov	0000	✓	✓
	0000	✓	✓		0000	✓	✓

The missing data was due to hardware outages at the DRSGS. This data set comprised the dependent sample predictands for the regression equation development.

An additional sample of satellite data was collected in November 1980. This data sample contained the same image sector and resolution as the November 1979 sample. Again data was selected at both 0000 GMT and 1200 GMT in order to correspond to the LFM forecast valid times. The November 1980 set was collected for use in testing the statistical significance of the multiple linear regression equations. Forty-nine image files were recorded on magnetic tape for the purpose.

Table 5 lists the corresponding dates and times of the data available for development and testing the regression equations for the ESP concept.

For case study applications of the ESP techniques three additional data sets were obtained in 1980. These data sets include GOES-East imagery taken at hourly intervals. Table 6 lists the inclusive dates and times of these three sets.

12 November 1980, 1200 GMT -- 19 November, 1800 GMT
24 November 1980, 2000 GMT -- 25 November, 2300 GMT
18 December 1980, 2200 GMT -- 20 December, 2300 GMT

Table 6: GOES-E data sets for ESP case study testing.

3.2.2 Satellite Data Reduction

The multiple linear regression equation development required the satellite imagery to be sampled at the LFM grid points. In this manner the LFM predictor variables for a given date-time-group and grid point would be regressed against the observed satellite IR temperature for the same date time group at the same grid point.

This required the satellite imagery to be earth located in order to reference the latitude and longitude of the LFM grid points. This was accomplished through the use of existing navigation software on the ADVISAR system. The navigation routines require one known earth reference point in both earth coordinates (i.e. latitude-longitude) and satellite coordinates (i.e. line-element). These, in conjunction with the orbit elements transmitted with the imagery, are used in an analytic method (Phillips and Smith, 1973) to determine display adjustments to earth locate the pixel elements.

A program was developed to determine the IR effective blackbody temperature of each grid point. It was decided to sample a region around each grid point rather than a single pixel value. The sample had to be smaller than the distance of adjacent grid points, but large enough to reflect the cloudiness which could be associated with the LFM variables. A 3 pixel by 3 pixel sample size was selected.

The entire 22 x 32 LFM grid locations displayed on a GOES-East image is depicted in Figure 2.

Due to the earth's curvature, as viewed from the geostationary satellite, it was felt that use of the western most grid points in the array would not represent valid mean temperature values. Therefore, the grid sampling array was a truncated version of the 22 x 32 LFM grid array. The array used is depicted in Figure 3. Each asterisk represents the location of the grid point. In the graphical representations of the grid on the satellite images each asterisk is 5 x 7 pixels in size, which is larger than the 3 x 3 pixel area sampled.

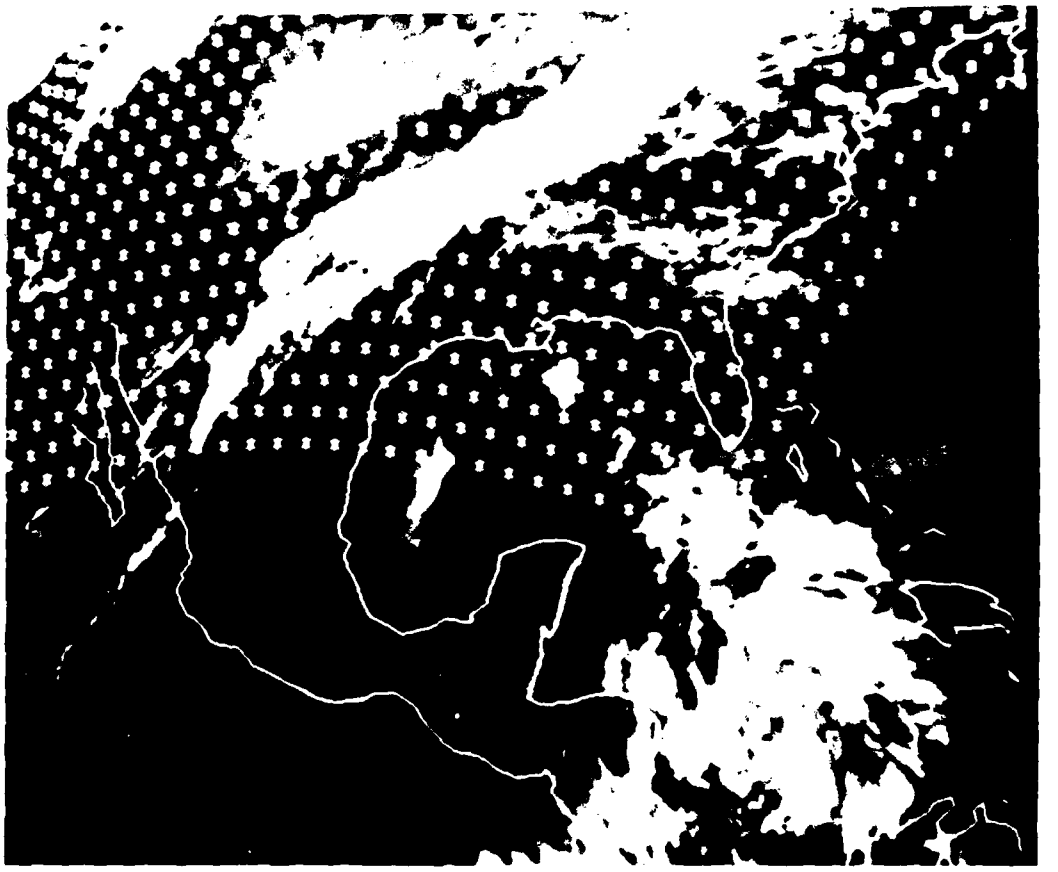

Figure 2. The 22 x 32 LFM grid array located on a digital satellite image display. The asterisk size is 5 x 7 pixels, larger than the 3 x 3 pixel area sampled for grid point temperatures.

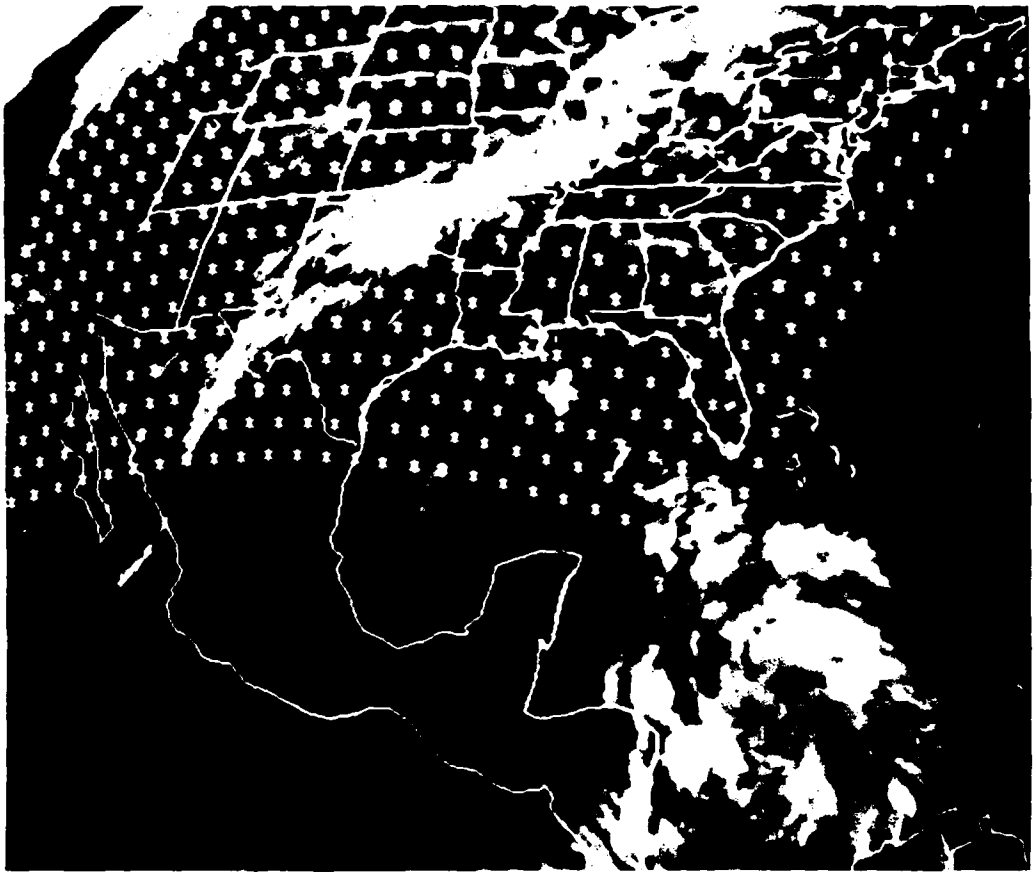

Figure 3. The 19 x 28 LFM grid point array used for digital satellite temperature analysis.

Each navigated image was displayed on the ADVISAR with the center screen resolution of .085° latitude per pixel and .112° longitude per pixel. This resolution correlates to approximately a 10 km x 10 km data representation at the center screen coordinate. Thus a 3 x 3 pixel sample represented a 30 km x 30 km area at the center of the image. Due to the variation in the satellite viewing angle at each grid point, the sample area was not constant. Table 7 summarizes the size of the 9 pixel region sampled at the extreme corners of the grid.

Table 7

Grid Location	East-West Sample Distance	North-South Sample Distance
Upper Left Corner	38.8 km	41.4 km
Upper Right Corner	32.8 km	27.9 km
Lower Left Corner	35.7 km	25.0 km
Lower Right Corner	27.6 km	24.0 km

The grid point temperature evaluation program was run for each image. The program stored the mean temperature of the 9 pixels sampled for each grid point. Grid boxes were evaluated on the northern border of the image (i.e. near scan line 200 approximately 50° N) if 5 or more pixels had digital satellite data.

Due to the western truncation and the lack of satellite data north of 50° N latitude, the grid analysis program derived 485 grid temperatures of the total 704 LFM grid points.

4.0 REGRESSION EQUATION DEVELOPMENT

4.1 System Selection

To facilitate the ease of the regression equation development, on existing statistics a computer library was used. Of the statistical libraries available, the Statistical Package of the Social Sciences (SPSS) was selected (Nie and Hall, et al., 1975). This package has inherent methods of handling missing values. This was an important consideration in the SPSS selection, since the LFM data sets contained missing LFM fields.

Additionally, the SPSS package had provisions for line deletion of variables entering the regression equations. Many of the variables calculated were not used, because the variable had to meet a specific criteria for inclusion as a predictor. For example, THRH required at least one of the high tropospheric levels to meet a criteria of relative humidity greater than or equal to 60%. If none of the three levels involved met the criteria, a flag value of 99999.0 was entered for the given grid point. In the regression development, this value either had to be considered "missing" or the 99999.0 would enter as a predicted temperature. This would, of course, bias the variable mean and would mask the meteorological significance of the variable.

Line deletion was selected as an option in the equation development, but several equations were developed at each level to account for "missing" data. This may be clarified by the following example. A regression equation has the form:

$$Y = A_0 + A_1 S_2 + A_2 X_2 + A_3 X_3 \ldots\ A_n X_n \qquad (5)$$

in which Y is the predictand, A_0 is the intercept, A_1 ... A_n are coeffectents and X_1 ... X_n are the variables entering the equation. Suppose that a derived equation for high cloud predictors had the forms:

$$Y_H = A_0 + A_1 \text{ THRH} + A_2 \text{ JETVAR} + A_3 \text{ KINDEX} + A_4 \text{ THWND} \quad (6)$$

where THRH, JETVAR, KINDEX and THWND are high cloud variables and A_1, A_2, A_3, and A_4 are their respective coefficients.

If a single equation was developed using the line deletion technique, only those grid points which had existing (i.e. non 99999.0) values would enter the sample from which the regression equation was developed. A cursory evaluation of the high cloud variables showed that the moisture variables selected had a high coincidence with observed high clouds in the satellite imagery. However, high moisture content was often not observed, therefore the majority of the grid points contained the flag value 99999.0. Similarly, high clouds were observed in many cases in which the LFM did not indicate high moisture, but other variables seemed to have a high prediction coincidence, i.e. the stability index and the thermal wind variable.

In an attempt to maximize the variables selected, it was decided to use a sequence of regression equations at each level. This was accomplished by selecting a set of predictor variables which included the moisture (non-continuous) variables. If a flag value was detected, i.e. 99999.0, then a series of additional predictors sets were used to develop several additional predictor equations which did not include a moisture flag value for that grid point. The final set of equations selected for testing were those that minimized the sample variance when used in combination.

4.2 Data Input

The satellite data and LFM predictor variables were used in regression development for the grid depicted in Figure 4.

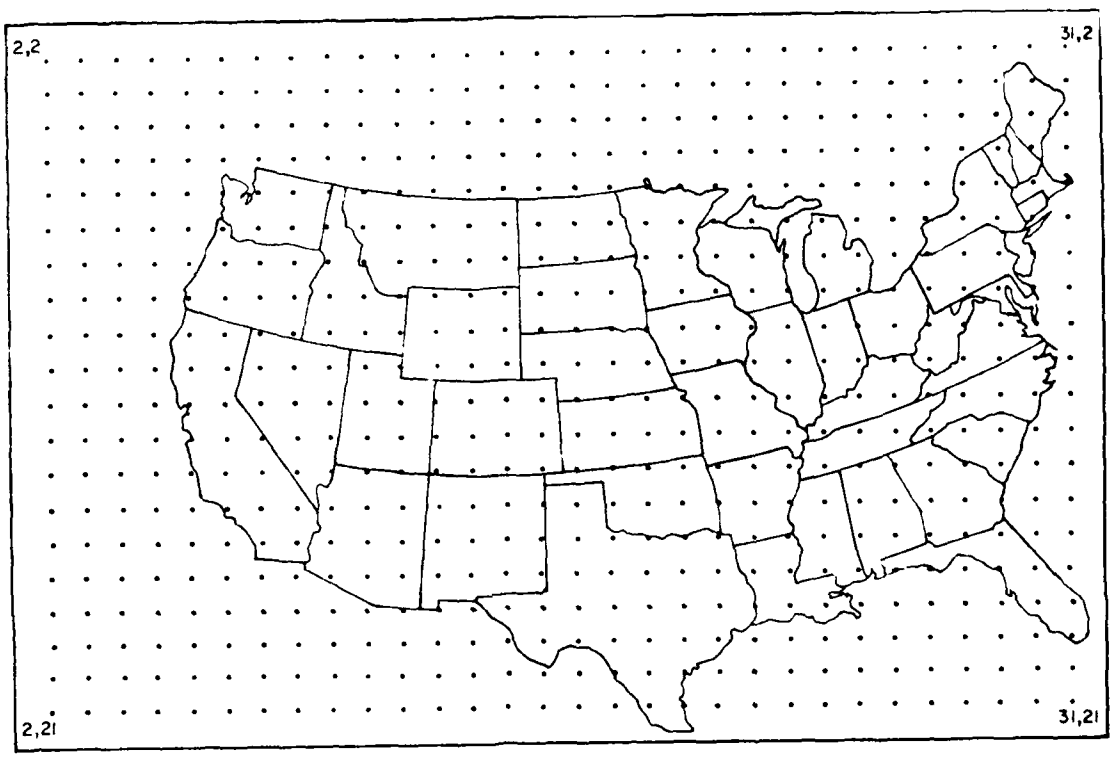

Figure 4. LFM grid points used in the regression analysis.

This grid contains 485 data points which cover most of the contiguous United States. Regression equations were developed using the satellite grid data derived from the grid analysis and the LFM forecasts valid at the corresponding times.

Due to missing data in both the LFM and satellite data sets, the various time periods (i.e. analysis 12 hr and 24 hr) had a different number of values entering the regression equations. Table 8 summarizes the data quantities entering into the equation development for each data type.

Table 8

Forecast Type	Number of Satellite Images with Corresponding LFM Forecasts	Number of Predictor Variables Used	Total Number of Variables Used to Derive the Equations
Initial	42	20	407,400
12 Hour Forecast	39	19	359,385
24 Hour Forecast	43	19	396,245

*This portion of the study has yet to be accomplished. Final statistical computational and image display work will be done by co-research personnel and transmitted to me for the final analysis.

5.0 USE OF THE ESP IN CASE STUDIES*

5.1 Objectives and Limitations

The final portion of this work will apply the developed regression equations to several case study meteorological situations. There are several questions which remain to be answered as to the true applicability of the ESP concept in light of many limitations. The following are known or suspected limitations inherent in the design of this study:

1) The sample of both the satellite and LFM data used to derive the equations may be too small to adequately reflect the value of the selected predictors in mesoscale applications.

2) The sample is totally derived from the month of November and, therefore, any applications should only be addressed to early winter (October, November, December) test cases.

3) Low clouds are difficult to discern from surface features when viewed by IR satellite imagery. This problem is suspected in the ESP applications, and may render the concept useless for dealing wih stratus and fog situations.

4) The resolution of the displayed ESP may be too course for adequate analysis in the ESP/satellite FOCAST mix. Further refinement of the ESP resolution can only be accomplished through more interpolation of the existing LFM grid size. This may induce many inaccuracies and "mask" the atmospheric situation as described by the LFM model.

5.2 Test Case Approach

In order to test the ESP/satellite mix in FOCASTing applications several case studies will be examined to determine the effect of the known or expected limitations on short range forecasts.

To accomplish this ESPs will be generated on the mesoscale window for the case studies. This window will be a 9 x 9 grid of the original LFM array. Figure 5 is an example of this grid overlayed on a GOES-East image.

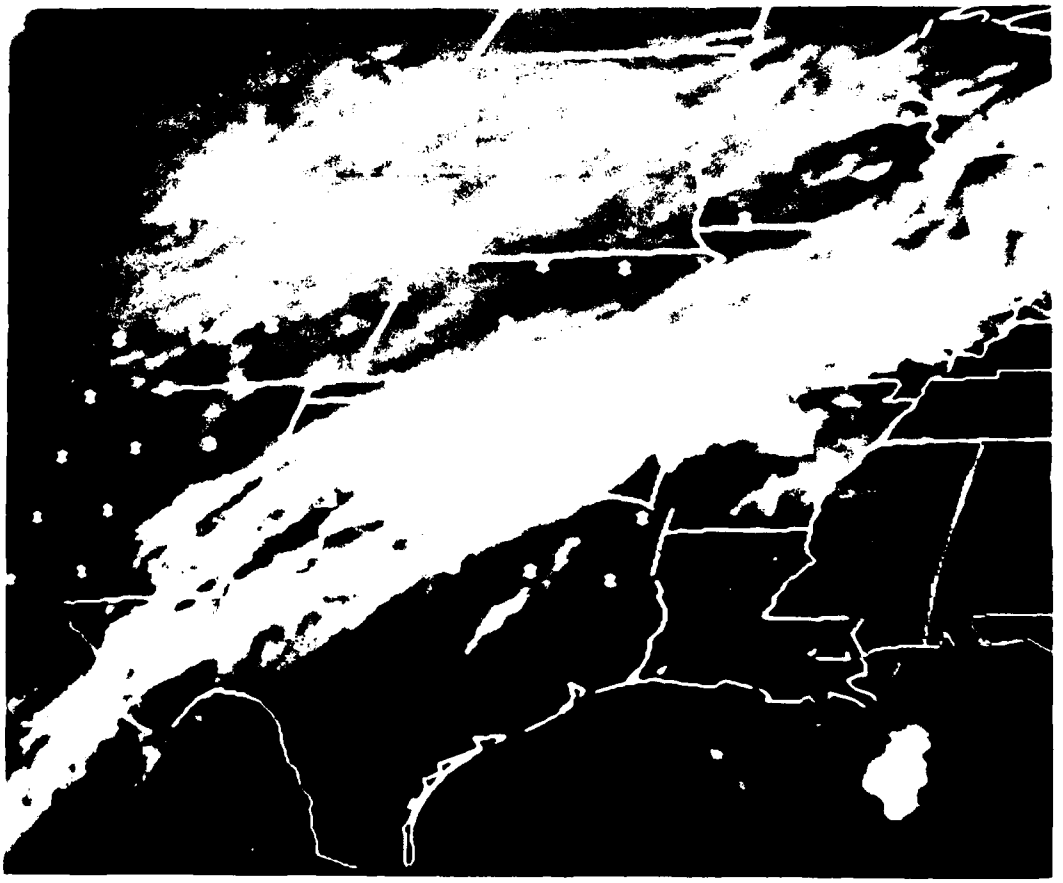

Figure 5.

To gain a better resolution of the displayed ESP, this 9 x 9 grid will be expanded to a 36 x 36 grid by interpolation to interior grid points as depicted in Figure 6.

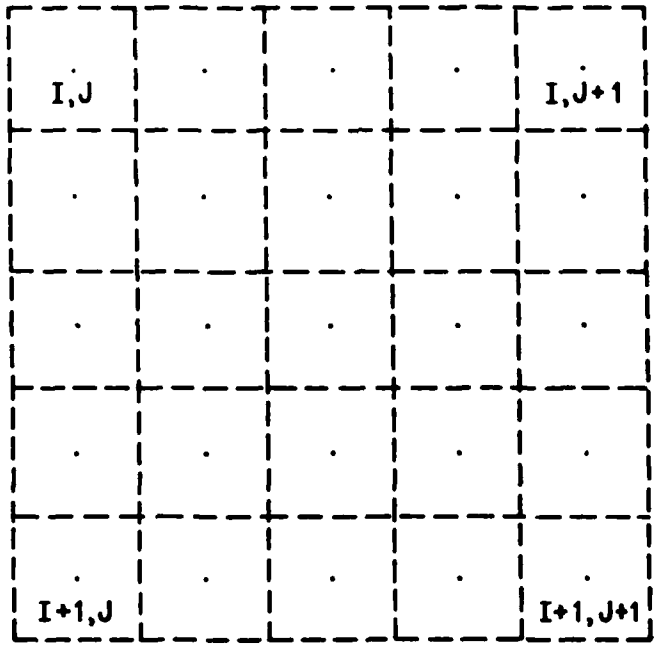

Figure 6. Interior grid points for meso-window ESP display. The I, J points designate the original LFM grid points and the additional points represent the interpolated field associated with the original four grid points.

In this manner the interpolated variables for each sub-LFM grid point will be entered into the regression equations. The resulting value will be graphically displayed for each point by an area of approximately 10x10 pixels, centered at the grid location.

Sequences of the ESPs in conjunction with satellite imagery and conventional observation will be used graphically to determine if the ESP has any value in determining the future occurance of meteorological criteria significant to terminal aviation forecasts. The following criteria are to be tests:

1) The onset/duration of precipitation.

2) The change in ceiling/visibility category for:

Category A	CIG $<$ 200 feet	and/or	VSBY $<$ 1/2 mile
Category B	200 $\leq$ CIG $<$ 1000	and/or	1/2 mile $\leq$ VSBY $<$ 2 miles
Category C	1000 $\leq$ CIG $<$ 3000	and/or	2 miles $<$ VSBY $<$ 3 miles
Category D	CIG $>$ 3000	and	VSBY $>$ 3 miles

These criteria are currently the verifying criteria for Air Weather Service TAFs and represent significant criteria to the aviation community.

REFERENCES

Anderson, R. K. et al., 1974: Application of Meteorological Satellite Data in Analysis and Forecasting, ESSA Technical Report NESC 51, Dept. of Commerce, March.

Anthony, R. W. and C. L. Bristor, 1978: Interactive System Requirements for the Realtime Demonstration of Mesoscale Weather Detection and Prediction. Preprints of Conference on Weather Forecasting and Analysis and Aviation Meteorology. AMS, Boston, MA, pp. 219-227.

Bellamy, J. C., 1949: Objective calculations of divergence, vertical velocity, and vorticity. Bull. Amer. Meteor. Soc., 30, 45-49.

Brown, J. A., 1977: Technical Procedures Bulletin No. 206: High Resolution LFM (LFM-II). Dept. of Commerce, NOAA, 4 p.

Conover, J. H., 1974: Specification of Current and Future Cloud Ceilings from Satellite Data. Preprint Fifth Conference on Weather Analysis and Forecasting, AMS, Boston, MA.

DeMasters, D. E. and M. L. Brown, 1979: Interactive Wind Analysis. Preprint DECUS 1979 Fall Symposium, San Diego, CA, December.

Ferguson, E. W. and M. D. Matthews, 1978: The Use of Satellite Imagery to Fine-Tune Numerical Guidance. Preprint Conference on Weather Analysis and Forecasting and Aviation Meteorology. AMS, Boston, MA, pp 245-250.

Haas, U. L. and T. A. Brubaker, 1979: Estimation of Lateral and Rotational Cloud Displacements from Satellite Pictures. AFGL-TR-0287, Air Force Geophysics Laboratory, Hanscom AFB, MA.

Hale, D., 1980: Personal Communication.

Hess, S. L., 1959: Introduction to Theoretical Meteorology. Chapter 4. Holt, Rinehart, and Winston, NY, 362 p.

Holton, J. R., 1979: An Introduction to Dynamic Meteorology. Chapters 3 and 4. Academic Press, NY, 391 p.

Jensenius, J. S., J. J. Cahir, and H. A. Panofsky, 1978: Estimation of outgoing longwave radiation rom meteorological variables accessible from numerical models. Quart. J. Roy. Met. Soc., 104, 119-130.

Johnson, R. H., 1976: The role of convective-scale precipitation downdraft in cumulus and synoptic scale interactions. J. Atmos. Sci., 33, 1890-1910.

Klein, W. H., 1978: An Introduction to the AFOS system. Preprint of Conference on Weather Analysis and Forecasting and Aviation Meterology. AMS, Boston, MA, pp. 186-189.

Kreitzburg, C. W., 1976: Interactive applications of satellite observations and mesoscale numerical models. Bull. Amer. Met. Soc., 57, 679-685.

Kruidenier, M. A., 1980: Mesoscale Organization of a Stratiform Cloud System Observed in Satellite Imagery. Master's Thesis. University of Washington, Dept. of Atmospheric Science, 138 p.

Leese, J. A., C. S. Novak, and B. B. Clark, 1971: An automated technique for obtaining cloud motion from geostationary satellite data using cross correlation. J. Atmos. Sci., 10, 118-132.

Lethbridge, M. and N. A. Panofsky, 1969: Satellite Radiation Measurements and Synoptic Data. Final Report, Grant No. WBG-48. Dept. of Meteorology, Pennsylvania State University.

List, R. J., 1966: Smithsonian Meteorological Tables. Page 370. Smithsonian Institution, Washington, DC, 527 p.

Muench, H. S., 1980: Local Forecasting through Extropolation of GOES Imaging Patterns. Preprints Eighth Conference on Weather Forecasting and Analysis, AMS, Boston, MA, 123-128.

Nagle, R. E. and J. R. Clark, 1968: An Approach to the SINAP Problem: A Quasi-Objective Method of Incorporating Meteorological Satellite Information in Numerical Weather Analysis. Final Report, Contract No. E-93-67(N), Met. Sat. Lab., NESC, ESSP, Dept. of Commerce.

Nie, N. H., 1975: SPSS - Statistical Package for the Social Sciences. McGraw Hill Book Co.

Phillips, D. and E. A. Smith, 1973: Geosynchronous Satellite Navigation Model. Studies of the Atmosphere Using Aerospace Probes, the University of Wisconsin Press, Madison, WI, 253-271.

Reynolds, D. W. and E. A. Smith, 1979: Detailed analysis of composited digital radar and satellite data. Bull. Amer. Met. Soc., 60, 1024-1037.

Reynolds, D. W., 1980: Observations of damaging hailstorms from geostationary satellite digital data. Mon. Wea. Rev., 108, 338-348.

Rieck, R. E., 1978: Technical Procedures Bulletin No. 232: The Limited-Area Fine Mesh Model (LFM). Dept. of Commerce, NOAA, 11 p.

Rieck, R. E., 1979: Technical Procedures Bulletin No. 269: Surface Topography Used in Operational NMC Prediction Models. Dept. of Commerce, NOAA, 8 p.

Sadowski, A. F. and R. E. Reick, 1977: Technical Procedure Bulletin No. 207: Stability Indices. Dept. of Commerce, NOAA, 6 p.

Shurman, F. G. and J. B. Hovermale, 1968: An operational six-layer primitive equation model. J. Atmos. Sci., 7, 525-547.

Sikula, G. J. and T. H. Vonder Haar, 1972: Very Short Range Local Area Weather Forecasting Using Measurements from Geosynchronous Meteorological Satellites. Atmospheric Science Paper No. 185, Dept. of Atmospheric Sciences, Colorado State University.

Smith, E. A. and D. R. Phillips, 1972: Automated Cloud Tracking Using Precisely Aligned Digital ATS Pictures. IEEE Transactions on Computers, C-21, pp. 715-729.

Smith, E. A. and T. H. Vonder Haar, 1980: Short Range Prediction of Satellite Cloud Pictures. Eighth Conference on Weather Forecasting and Analysis, AMS, Boston, MA.

Smith, P. J. and C. Ping Lin, 1978: A comparison of synoptic-scale-vertical motions. Computed by the kinematic method and two forms of the omega equation. Mon. Wea. Rev., 106, 1687-1694.

Starr, D. and S. K. Cox, 1980: Characteristics of Middle and Upper Tropospheric Clouds as Deduced from Rawinsonde Data. Atmospheric Science Paper No. 327, Dept. of Atmospheric Science, Colorado State University.

Starr, D., 1981: Personal Communications.

Stackpole, J., 1970: Technical Procedures Bulletin No. 57: Revised Method of 1000 MB Height Computation in the PE Model. Dept. of Commerce, NOAA, 6 p.

Suchman, D., B. Auvine, and B. Hinton, 1978: The Use of an Interactive Computer System in Applied Meteorological Forecasting. Preprint Conference on Weather Analysis and Forecasting and Aviation Meteorology, AMS, Boston, MA, pp. 215-218.

Vonder Haar, T. H., E. A. Smith, and R. W. Reynolds, 1977: Use of Quantitative Satellite Data for Objective Mesoscale Weather Forecasting. A Research Proposal to Air Force Geophysics Laboratory, November.

Wash, C. H., J. Stremikis, and D. R. Johnson, 1979: Objective Forecasts of Subsynoptic Convective Areas Using Interactive Computer Systems. Preprint Eleventh Conference on Severe Local Storms, AMS, Boston, MA, pp. 580-586.

Wash, C. H. and T. M. Whittaker, 1980: Subsynoptic analysis and forecasting with an interactive computer system. Bull. Amer. Met. Soc., 61, 1584-1591.

Wilson, G. S., 1979: Medium Range Forecasting on Thunderstorm Location and Severity Using Regional-Scale Atmospheric Structure and Dynamics Predicted by the LFMZ Model. Preprint Eleventh Conference on Severe Local Storms, AMS, Boston, MA, pp. 593-599.

APPENDIX A

LFM OUTPUT PREDICTORS

A. Low Cloud Tops

1. Variable: The temperature of a level as a function of low dew point depression at that level

   Variable Name: TLDP

   Variable Type: Continuous

   Cut off Value: Dew point depression less than or equal to $5^{o}K$

   Vertical Stratification: The lowest pressure level with a dew point depression of $5^{o}K$ or less from 700 mb to 1000 mb

   Non-Criteria Value: The surface temperature of the grid point derived from an environmental lapse rate, calculated from the 1000 mb temperature and height values to the elevation of the grid point

   Input data: 1000 mb temperature
   1000 mb dew point temperature
   850 mb temperature
   850 mb dew point temperature
   700 mb temperature
   700 mb dew point temperature
   1000 mb height
   grid point elevation

2. Variable: The temperature of a level as a function of high relative humidity at that level

   Variable Name: TLRH

   Variable Type: Continuous

   Cut off Value: Relative humidity greater than or equal to 60%

   Vertical Stratification: The lowest pressure level with a relative humidity of 60% or greater from 700 mb to 1000 mb.

   Non-Criteria Value: The surface temperature of the grid point derived from an environmental lapse rate, calculated from the 1000 mb temperature and height values to the elevation of the grid point

In-Put data: 1000 mb temperature
1000 mb dew point temperature
850 mb temperature
850 mb dew point temperature
700 mb temperature
700 mb dew point

3. Variable: Vertical motion at 850 mb and 700 mb

Variable Name: OMEGA 2 and OMEGA 3

Variable Type: Continuous

Input data: u wind component from
1000 mb to 250 mb
v wind component from
1000 mb to 250 mb

4. Variable: A combination of vertical motion and relative humidity at 850 mb

Variable Name: OMEGRHL

Variable Type: Continuous

Input Data: u wind component from
1000 mb to 250 mb
v wind component from
1000 mb to 250 mb

5. Variable: The interpolated temperature of a layer in which the lower level has a high relative humidity depression and the higher level has a low relative humidity.

Variable Name: TOPDRYL

Variable Type: Continuous

Cut-off Value: Relative humidity for the lower pressure level greater than or equal to 60% and relative humidity of the higher level less than 60%

Non-criteria Values: The surface temperature of the grid point.

Input Data: 1000 mb temperature
1000 mb dew point temperature
850 mb temperature
850 mb dew point temperature
700 mb temperature
700 mb dew point temperature

6. Variable: The "k" stability index

   Variable Name: KINDEX

   Variable Type: Continuous

   Input Data: 850 mb temperature
   850 mb dew point temperature
   700 mb temperature
   700 mb dew point temperature
   500 mb temperature

7. Variable: The advection of low level moisture derived from the mean μ and ν wind components and the mean relative humidity from 1000 mb to 700 mb

   Variable Name: MOISADV

   Variable Type: Continuous

   Input Data: 1000 mb temperature
   1000 mb dew point temperature
   1000 μ wind component
   1000 ν wind component
   850 mb temperature
   850 mb dew point temperature
   850 μ wind component
   850 ν wind component
   700 mb temperature
   700 mb dew point temperature
   700 μ wind component
   700 ν wind component

B. Middle Cloud Predictors

1. Variable: The temperature of a level as a function of low dew point depression.

   Variable Name: TMDP

   Variable Type: Non Continuous

   Cut-off Value: Dew point depression less than or equal to $5^{o}k$

   Vertical Stratification: The lowest pressure level with a dew point depression of $5^{o}K$ or less from 500 mb to 700 mb.

   Non Criteria Value: 99999

Input Data: 700 mb temperature
700 mb dew point
500 mb temperature
500 mb dew point

2. Variable: The temperature of a level as a function of high relative humidity at that level.

Variable Name: TMRH

Variable Type: Non Continuous

Cut-off value: Relative humidity greater than or equal to 60%

Vertical stratification: The lowest pressure level with a relative humidity of 60% or greater from 500 mb to 700 mb

Non-Criteria Value: 99999.0

Input Data: 700 mb temperature
700 mb dew point
500 mb temperature
500 mb dew point

3. Variable: Vertical motion at 700 mb and 500 mb

Variable Name(s) OMEGA3, OMEGA4

Variable Type: Continuous

Input Data: u wind components from
1000 mb to 250 mb
v wind components from
1000 mb to 250 mb

4. Variable: A combination of vertical motion and moisture at 700 mb

Variable Name: OMEGRHM

Variable Type: Continuous

Input Data: u wind component from 1000 mb to 250 mb
v wind component from 1000 mb to 250 mb
700 mb temperature
700 mb dew point temperature

5. Variable: The interpolated temperature of a layer in which the low level has a high relative humidity and the higher level has a low relative humidity.

Variable Name: TOPDRYM

Variable Type: Non-Continuous

Cut-off Value: Relative humidity for the lower pressure level (700 mb) greater than or equal to 60% and relative humidity at the higher pressure level (500 mb) less than 60%.

Non Criteria Values: 99999

Input Data: 700 mb temperature
700 mb dew point temperature
500 mb temperature
500 mb dew point temperature

6. Variable: The "k" stability index

Variable Name: KINDEX

Variable Type: Continuous

Input Data: 850 mb temperature
850 mb dew point temperature
700 mb temperature
700 mb dew point temperature
500 mb temperature

7. Variable: Thermal wind magnitude for the layers from 850 mb to 500 mb.

Variable Name: THWND

Variable Type: Continuous

Input Data: 500 mb geopotential heights
850 mb geopotential heights

C. High Cloud Predictors

1. Variable: The temperature of a level as a function of low dew point depression.

Variable Name: THDP

Variable Type: Non-continuous

Cut-off Value: Dew point depression less than or equal to $5^{o}K$ at 500 mb and dewpoint depressions less than or equal to $10^{o}K$ at 400 mb and 300 mb.

Vertical Stratification: The lowest pressure level with a dew point depression less than or equal to the above mentioned criteria.

Non-Criteria Value: 99999

Input Data: 500 mb temperature
500 mb dew point temperature
400 mb temperature
400 mb dew point temperature
300 mb temperature
300 mb dew point temperature

2. Variable: The temperature of a level as a function of high relative humidity.

Variable Name: THRH

Variable Type: Non Continuous

Cut-off Value: Relative humidity with respect to ice greater than or equal to 60%.

Vertical Stratification: The lowest pressure level with a relative humidity greater than or equal to 60%.

Non Criteria Value: 99999.0

Input Data: 500 mb temperature
500 mb dew point temperature
400 mb temperature
400 mb dew point temperature
300 mb temperature
300 mb dew point temperature

3. Variable: The interpolated temperature of a layer in which the lower level has a high relative humidity with respect to ice and the high level has a low relative humidity with respect to ice.

Variable Name: TOPDRYH

Variable Type: Non-Continuous

Cut-off Value: Relative humidity for the lower level greater than 60% and the relative humidity for the upper level less than 60%.

Vertical Stratification: The lowest pressure level with meeting the above criteria.

Non-Criteria Value: 99999.0

Input Data: 500 mb temperature
500 mb dew point temperature
400 mb temperature
400 mb dew point temperature
300 mb temperature
300 mb dew point temperature

4. Variable: Vertical motion at upper tropospheric levels

Variable Name: OMEGA 4, OMEGA 5, OMEGA 6

Variable Type: Continuous

Input Data: u wind components from
1000 mb to 250 mb
v wind components from
100 mb to 250 mb

5. Variable: The "k" stability index

Variable Name: KINDEX

Variable Type: Continuous

Input Data: 850 mb temperature
850 mb dew point temperature
700 mb temperature
700 mb dew point temperature
500 mb temperature

6. Variable: The thermal wind magnitude computed for the layers 850 mb through 500 mb.

Variable Name: THWND

Variable Type: Continuous

Input Data: 500 mb - geopotential heights
850 mb - geopotential heights

7. Variable: A parameter to estimate jet stream cirrus basids on the magnitude of the 300 mb wind and the sign of vorticity at 300 mb.

Variable Name: JETVAR

Variable Type: Non-Continuous

Cut-off Criteria: The magnitude of 300 mb winds greater than or equal to 35 m/s and the sign of the relative vorticity negative.

Non Criterial Value: 99999.0

Input Data: 300 mb u wind component
300 mb v wind component

8. Variable: A combination of vertical motion and moisture at 500 mb

Variable Name: OMEGRHH

Variable Type: Continuous

Input Data: u wind components from 1000 mb to 250 mb
v wind components from 1000 mb to 250 mb

Appendix B

Equation Derivation

1. Dew Point Depression

Dew Point Depression is defined as

$$\text{Dew Point Depression} = T - T_d \tag{B1}$$

This value must always be greater than or equal to 0.0, however a preliminary check of the LFM output revealed some small discrepancies in which the dew point was slightly larger than the temperature at a given level. A close analysis of these situations revealed that when a negative dew point depression occurred, it was surrounded by grid values close to or equal to zero. Therefore, a line of code was added to the data reduction program to set the dew point depression equal to 0.0 if the negative dew point depression situation occurred. It is believed that this erroneous output is caused by the interpolation of the relative humidity and temperature fields from the sigma layers to the pressure layers in the LFM model.

2. Relative Humidity

Relative humidity is defined, (Hess, 1959) by

$$RH = \frac{w}{w_s} \tag{B2}$$

$$\text{where } W_s = \frac{\epsilon e_s}{p - e_s} \approx \frac{\epsilon e_s}{p} \tag{B3}$$

$$\text{and } W = \frac{\epsilon e}{p - e} \approx \frac{\epsilon e}{p} \tag{B4}$$

Substituting equations B3 and B4 into B2 yields:

$$RH = \frac{e}{e_s} \tag{B5}$$

The Clapyron equation may be expressed in the integrated form (with T in ^{o}k and d_s in mb)

$$\ln\left(\frac{e_s}{6.11}\right) = \frac{\epsilon L}{R_d}\left(\frac{1}{273} - \frac{1}{T}\right) \tag{B6}$$

$$e_s = 6.11 \exp\left[\frac{\epsilon L}{R_d}\left(\frac{1}{273} - \frac{1}{T}\right)\right] \tag{B7}$$

Similarly,

$$e = 6.11 \exp\left[\frac{\epsilon L}{R_d}\left(\frac{1}{273} - \frac{1}{T_D}\right)\right] \tag{B8}$$

By substituting B6 and B7 into Equation B5 yields

$$RH = \exp\left[\frac{\epsilon L}{R_d}\left(\frac{1}{T} - \frac{1}{T_D}\right)\right] \tag{B9}$$

Relative humidity was calculated with respect to ice for the 500 mb, 400 mb, and 300 mb layers. Starr (1981) derived the following expression from tables given by List (1966).

$$RH_i = RH_w * (A\phi + (T * (A1 + T * A2)) \tag{B10}$$

where

A = 0.9994533

A1 = -0.9806515 E-02

A2 = 0.50993939 E-04

T is in units of °C

3. Vertical Motion

The kinematic method (Bellamy, 1949) was used in calculating the vertical motion fields for the initial, or observed, LFM data set. The kinematic method has potential for large errors due to inaccurate wind values (Holton, 1979), was a primary consideration in using the kinematic method. Smith and Ping Lin (1978) compared synoptic scale vertical motions computed by the kinematic method and two forms of the omega equation. Their results indicated no significant advantage to any of the three methods. However, the kinematic values were more compatable to cloud and precipitation occurances than the omega equation values.

Vertical velocities were computed by

$$\omega(p_1) = \omega(p_o) + \int_{p_1}^{p_o} \overline{(\nabla \cdot \mathbb{V})}_c \, dp \qquad \text{(B11)}$$

where $(\nabla \cdot \mathbb{V})_c$ is the corrected mean divergence of the levels in question; p_0 and p_1, given by

$$\overline{(\nabla \cdot \mathbb{V})}_c = \overline{\nabla \cdot \mathbb{V}} - \frac{1}{p_s - p_T} \int_{p_T}^{p_s} \nabla \cdot \mathbb{V} \, dp \qquad \text{(B12)}$$

In this manner the vertical velocity vanishes at p_S, the surface 1000 mb level, and p_T, the tropopause level (Johnson, 1976). In this computation p_T was assumed to be 250 mb which represents a logical tropopause level for the early winter season, and p_s was taken as 1000 mb.

The divergence fields were determined by using the finite difference approximation from the u and v wind component fields, Holton (1979), by use of Equation B13.

$$\frac{u}{x} + \frac{v}{y}_{I,J} \simeq \frac{u(I,J+1) - v(I,J-1)}{2*D} + \frac{v(I,1,J) - u(I,J+1,J)}{2*D} \qquad \text{(B13)}$$

where the grid points are dimensioned as in Figure B1

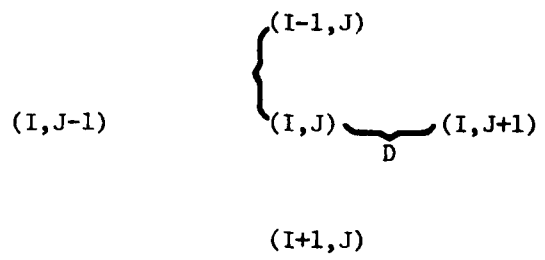

Figure B1

The grid distance, D, was computed for each grid interval by use of the appropriate map factor for the polar sterographic grid (Tech. Procedures Bulletin No. 232 1973). The equation used for the grid resolution was

$$D(km) = 1.90 \times 10^5 \times \frac{\sin\phi + 1.0}{\sin 60° + 1.0} \qquad \text{(B14)}$$

where ϕ, the latitude, was given by (Hale, 1980)

$$\phi(\text{degrees}) = 90.0 - 2* \arctan (R/RE) *5.2958 \qquad \text{(B15)}$$

where:

$$RE = 62.417325 \qquad \text{(B16)}$$

$$R = \sqrt{(J-15)^2 + (I + 17)^2} \qquad \text{(B17)}$$

In equation B17, the I and J values correspond to the appropriate I,J coordinate of the WPRS 22 by 32 LFM grid.

4. K Index

The K stability index is defined as (Technical Procedures Bulletin. No. 207):

$$K = T_{850} + T_{D_{850}} - (T_{700} - T_{D_{700}}) - T_{500} \tag{B18}$$

5. Thermal Wind

The magnitude of the thermal wind was calculated from (Holton, 1979):

$$V_T = \sqrt{u_T^2 + v_T^2} \tag{B19}$$

where

$$u_T = -\frac{1}{f}\frac{\partial}{\partial y}\left(\phi_{500} - \phi_{850}\right) \tag{B20}$$

$$v_T = \frac{1}{f}\frac{\partial}{\partial x}\left(\phi_{500} - \phi_{850}\right) \tag{B21}$$

6. Relative Vorticity

Relative vorticity was calculated using the finite difference form of

$$\zeta \equiv \frac{\partial v}{\partial x} - \frac{\partial u}{\partial y} \tag{B22}$$

or

$$\zeta(I,J) \equiv \frac{v(I,J+1) - v(I,J-1)}{2*D} - \frac{u(I-1,J) - u(I+1,J)}{2*D} \tag{B23}$$

using similar I,J subscripts as in Figure B1.

END

DATE
FILMED
4-82

DTIC